

## Magnetic Hysteresis Dynamics: Thin $p(1 \times 1)$ Fe Films on Flat and Stepped W(110)

Jih-Shin Suen and J. L. Erskine

*Department of Physics, University of Texas at Austin, Austin, Texas 78712*

(Received 28 June 1996)

Hysteresis properties of ultrathin (1.5–4 monolayer) epitaxial Fe films grown on flat and stepped W(110) surfaces are studied as a function of film thickness, temperature, and the strength and frequency of the applied sinusoidal magnetic field. Power law scaling of the hysteresis loop area is observed over five decades in frequency. Measured exponents depart significantly from those reported based on prior experiments and existing theoretical models. An abrupt transition from switching behavior to a stable magnetic state is observed at a critical frequency where the dynamic coercivity exceeds the applied field strength. [S0031-9007(97)03008-1]

PACS numbers: 75.60.Ej, 75.40.Gb, 75.70.Ak

The dynamics of magnetization reversal has recently attracted considerable scientific interest based on new opportunities to explore concepts of universality and scaling [1–12]. Theoretical efforts have explored hysteresis phenomena in model magnetic systems based on a variety of approaches [1–10]. A general objective of these efforts has been to discover scale-invariant descriptions of the energy loss per cycle (area of the hysteresis loop) as a function of external parameters (applied magnetic field strength  $H$ , frequency  $\Omega$ , and temperature  $T$ ) and intrinsic system parameters (dimensionality and symmetry, i.e., magnetic anisotropy). For example, in the low frequency limit, invariant functions of the hysteresis loop area have been shown to reduce to a power law function of the form [5]

$$A \propto H^\alpha \Omega^\beta T^{-\gamma}, \quad (1)$$

where  $\alpha$ ,  $\beta$ , and  $\gamma$  are exponents that depend on the dimensionality and symmetry of the system. Two basic types of dynamical models have been explored theoretically: Ising-like models [4–6,9] in which an energy barrier separates the two equivalent magnetized states, and continuous spin models [1–4,7,8] having no barrier. Specific values of the exponents in Eq. (1) for various models are summarized in Table I with corresponding references to the literature.

Dynamical properties of magnetization reversal have also been investigated experimentally in ultrathin film systems [11–14]. These systems offer unique opportunities to explore dynamical effects in well-characterized structures in which relevant intrinsic parameters (dimensionality, anisotropy) can be controlled. Studies of Fe on Au(001) [11] and Co on Cu(001) [12] have apparently revealed dynamical scaling effects corroborating general theoretical predictions based on the continuous spin and Ising-like models: power law scaling of the loop area (exponents in Table I); constant loop area characteristic of adiabatic magnetization reversal at very low frequencies [12]; and threshold field effects associated with a double-well barrier in Ising-type models.

In this Letter, we report hysteresis loop measurements of well-characterized ultrathin Fe films grown on flat and stepped W(110) surfaces as a function of  $H$ ,  $\Omega$ , and  $T$ . Our results are consistent with universal behavior (thickness invariant exponents) and clearly exhibit uniform power law scaling over the entire range of  $\Omega$  and  $H$  currently accessible by our experiments. However, our experimental results are incompatible with the experimental and theoretical values of dynamic scaling exponents listed in Table I. We also observe an abrupt collapse of the hysteresis loop at critical frequencies governed by the condition  $H_c^* > H$  where  $H_c^*$  is the dynamic coercive force. This abrupt change is qualitatively different from the frequency-dependent evolution of hysteresis loop shapes predicted by Monte Carlo simulations based on Ising models [1,3,6] and reported in prior experiments [11,12].

Vacuum deposited ultrathin Fe films on W(110) were selected for our experiments because this system is a nearly ideal and extensively studied 2D magnetic system [15]. The Fe films on W(110) exhibit uniaxial anisotropy [110] (easy direction) and yield power law behavior [15] for  $M(T) \propto (T_c - T)_T^\beta$  (near the Curie temperature  $T_c$ ) which is governed by an exponent very close to the 2D Ising model value  $\beta_T = \frac{1}{8}$ .

Our thin films were grown at deposition rates of approximately 0.7 ML per min and were studied in ultrahigh vacuum ( $P \sim 3 \times 10^{-11}$  torr;  $2 \times 10^{-10}$  torr during film growth). Film thickness was monitored by a quartz microbalance placed approximately  $\frac{1}{5}$  the source-to-sample distance. LEED and Auger analysis were used to characterize structure, check consistency of thickness calibrations with other reported work for  $2 \leq \Delta X \leq 9$  ML thickness, and to monitor film purity. The W(110) crystal was bifacial with one face cut within  $\frac{1}{2}$  of the [110] crystallographic direction and the second face cut  $6.3^\circ$  off the [110] axis to produce uniform 28 Å terraces as measured by splitting the LEED spots. Cleaning procedures were similar to those described in prior publications [16].

TABLE I. Dynamic scaling exponents for 2D and 3D continuum and Ising model systems. [Refer to Eq. (1)].

		$\alpha$	$\beta$	$\gamma$
Continuum models:				
3D $(\Phi^2)^3$ :	Ref. [1]	2/3	1/3	$1.00 \pm 0.03$
	Ref. [7]		$1/2^a$	
3D $(\Phi^2)^2$ :	Ref. [1]	$0.66 \pm 0.05^a$	$0.33 \pm 0.03^a$	0.7
2D $(\Phi^2)^2$ :	Ref. [3]	$0.47 \pm 0.02$	$0.40 \pm 0.01$	
	Ref. [7]	1/2	1/2	
3D O(N):	Ref. [2,4]	1/2	1/2	
1D:	Ref. [8]		2/3	
Ising models:				
3D (MC):	Ref. [5]	$\sim 0.67$	$\sim 0.45$	$\sim 1.98$
2D (MC):	Ref. [5]	$\sim 0.70$	$\sim 0.36$	$\sim 1.18$
	Ref. [6]	$0.46 \pm 0.05$	$0.36 \pm 0.06$	
	Ref. [4]	$\sim 1/2^b$	$\sim 1/2^b$	
	Ref. [9]	2/3	2/3	
Experiments:				
Fe/Au(001):	Ref. [11]	$0.59 \pm 0.07$	$0.31 \pm 0.05$	
Co/Cu(100):	Ref. [12]	$0.67 \pm 0.01$	$0.66 \pm 0.03$	

<sup>a</sup>Temperature independent.<sup>b</sup>Temperature dependent.

Hysteresis loops were measured *in situ* using the magneto-optic kerr effect (MOKE). An in-vacuum laminated-core (stack of 14 mil thick HyMu80 laminations) electromagnet was constructed to reduce eddy current losses and extend the loop tracer frequency response. Precise knowledge of magnetic field strength at the sample and phase shifts introduced by the magnet and/or signal processing instrumentation is required to obtain meaningful results for dynamic hysteresis effects. Our approach to calibrating the MOKE polarimeter was to measure the Faraday effect from a small glass prism placed at the sample position.

Figure 1 displays a selection of  $\Omega$ -dependent hysteresis loops. The applied magnetic field was parallel to the (uniaxial) easy magnetization direction of both the flat and stepped surface (inset of Fig. 1). No evidence of a temperature- or thickness-dependent reorientation transition (change of magnetic symmetry) was observed on either the flat or stepped surface. Both flat and stepped surfaces yielded similar magnetic behavior.

The shape of the hysteresis loops for  $H$  near switching thresholds was found to depend on the area of the surface probed by the laser. Similar effects have been reported and discussed in relation to studies of domain wall nucleation and motion in amorphous rare earth-transition metal thin films [17]. An unfocused laser beam (nominal diameter  $\sim 1$  mm) yielded hysteresis loops having slightly rounded corners particularly at higher frequencies. Hysteresis loops measured with a focused laser beam (diameter  $\sim 50$   $\mu$ m) maintained their square shape. This behavior can be understood in terms of the average domain size during magnetization reversal in relation to the probed area. A detailed study and analysis of these effects will be

presented in a separate publication; here we simply state that over the range of parameters studied, the measured loop areas depend only on the (temperature-dependent) saturation magnetization and the dynamic coercive force  $H_c^*$ , and do not appear to be a function of the rather small variations in loop shape vs laser spot size on the sample. The probed area scale dependence of measured

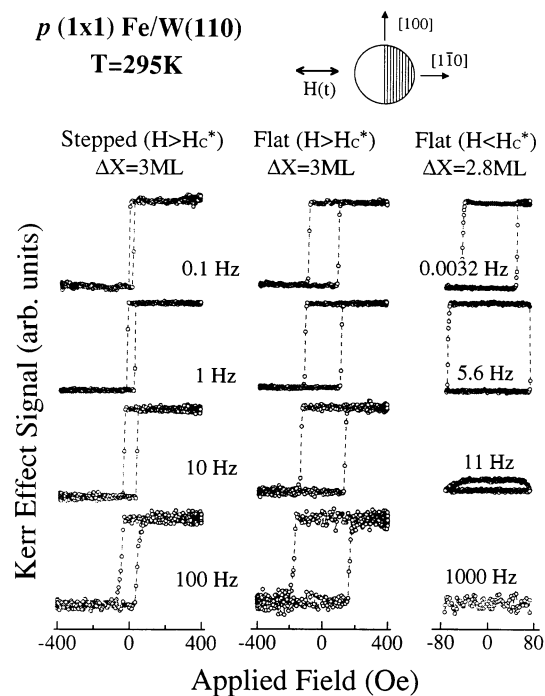


FIG. 1. Typical hysteresis loops from  $p(1 \times 1)$  Fe films on W(110). Inset, upper right, shows orientation of applied field in relation to steps and crystallographic axes.

loops in our experiments suggests that the reversal mechanism for  $p(1 \times 1)$  Fe on W(110) films involves creation of domains on a scale of  $\sim 100 \mu\text{m}$ .

Log-log plots of hysteresis loop area  $A$  as a function of  $\Omega$  for selected values of film thickness, temperature, and applied field strength are shown in Fig. 2 (flat surface) and Fig. 3 (stepped surface). All loops obtained using  $H > H_c^*$  yield power law dependence over the accessible frequency range. For lower values of  $H$ , and when  $\Omega$  reached a value where  $H_c^* > H$ , an abrupt collapse of the loop occurred (Figs. 2 and 3) in which the film would remain in one of the equivalent (single domain) states. Plots of  $H_c^*(\Omega, T)$  vs  $\ln(H)$  (not shown but apparent from Figs. 2 and 3) reveal that the measured coercive fields of our films are strongly temperature dependent. Specifically, at low  $\Omega$ ,  $H_c(100 \text{ K}) \cong 3H_c(300 \text{ K})$  for both smooth and stepped films of a given thickness suggesting first order  $kT$  dependence. More extensive temperature-dependent data are required to critically test theoretical models [i.e., Eq. (8) of Ref. [14]], but the strong temperature dependence and uniform power law behavior displayed in Figs. 2 and 3 are strong evidence that our experiments are probing dynamics response of the films over the entire frequency range.

In favorable cases (when  $H_c^*$  was suitably small) power law behavior was observed over nearly five decades of frequency (0.0032 Hz to 1 kHz). The exponent  $\beta$  in Eq. (1)

has been calculated from the experimental data in Figs. 2 and 3 and displayed in the figures. Many films have been studied ( $1.5 \leq \Delta X \leq 4 \text{ ML}$ ) and the exponent  $\beta$  follows the behavior indicated in the two figures. On the flat surface, the exponent appears to be independent of film thickness and applied magnetic field strength (provided  $H > H_c^*$ ) even though  $H_c^*$  varies strongly with  $\Delta X$  (compare 3.0 ML, 2.8 ML; Fig. 1, Fig. 2). This suggests universal behavior of some type. The difference in  $\beta$  at  $T = 295 \text{ K}$  between the 3 ML film on the flat and stepped surface can be considered a real effect since the same film was studied on the double-faced crystal and the difference (flat surface  $\beta = 0.063 \pm .002$ , stepped surface  $\beta = 0.076 \pm .002$ ) is considerably larger than the error bars. This suggests that step-induced film roughness plays a role in domain wall dynamics. From Fig. 3 it is clear that the films grown on the stepped surface also exhibit the abrupt collapse of loop area when  $H_c^* > H$ , but seem to also exhibit slight thickness-dependent decrease in the parameter  $\beta$ . More precise measurements of the loop collapse, which will be discussed in a future paper, suggest power law behavior exists, and could be related to discontinuous double-power-law scaling [9] that occurs in the kinetic Ising model.

Figure 4 displays a set of  $H$  dependent hysteresis loops at constant  $\Omega$  and fixed temperature along with a log-log plot of the loop area vs  $H$ . This data yields a value for the parameter  $\alpha = 0.254 \pm 0.003$  in Eq. (1) and also shows

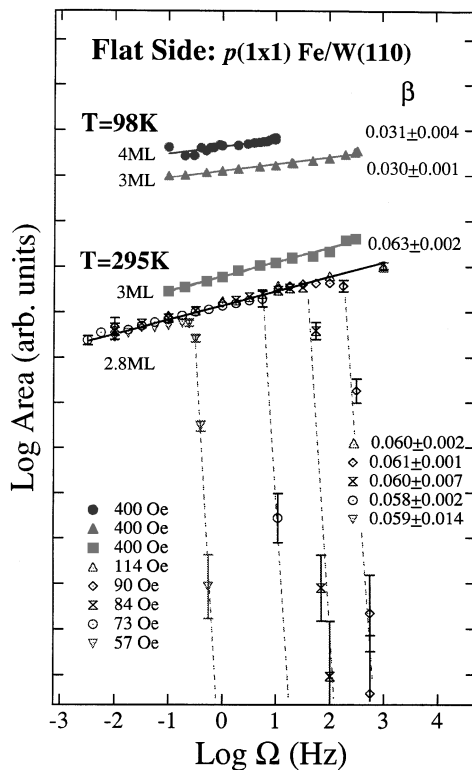


FIG. 2. Log-log plots of hysteresis loop area  $A$  vs frequency  $\Omega$  for  $p(1 \times 1)$  Fe on flat W(110) two temperatures for various film thickness and applied field strengths. The parameter  $\beta$  (slope of line) is tabulated. Dashed lines show collapse of loop for  $H_c^* > H$ .

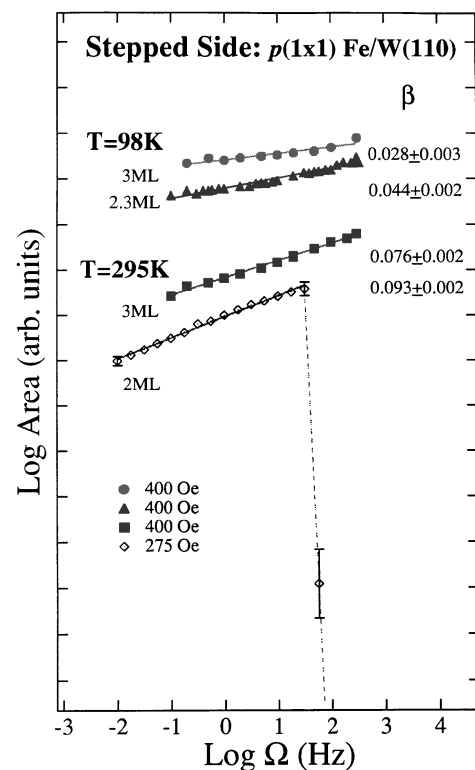


FIG. 3. Log-log plots of hysteresis loop area  $A$  vs frequency  $\Omega$  for  $p(1 \times 1)$  Fe on stepped W(110) at two temperatures for various film thickness and applied field strengths. The parameter  $\beta$  (slope of line) is tabulated. Dashed line shows collapse of loop for  $H_c^* > H$ .

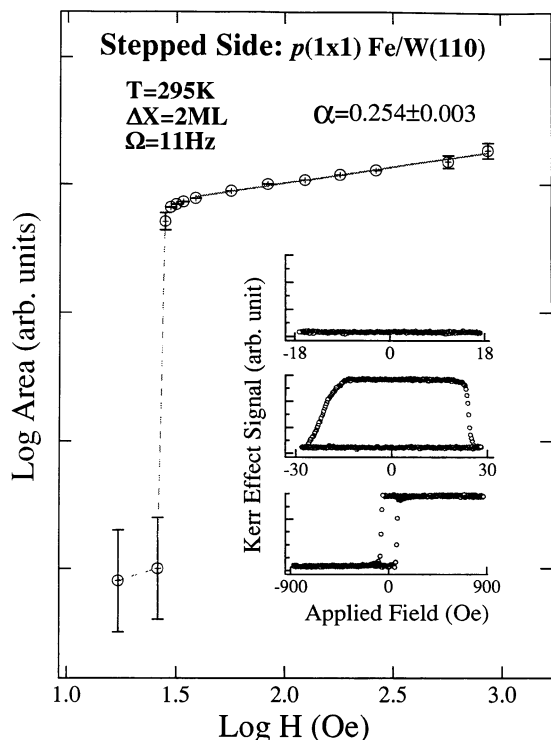


FIG. 4. Log-log plot of hysteresis loop area  $A$  vs applied field strength  $H$  at fixed  $\Omega$  showing abrupt transition to switching behavior at  $H > H_c^*$ . Slope of line for  $H > H_c^*$  yields exponent  $\alpha$ .  $H$ -dependent loop area offsets in Fig. 3 (which are not apparent) are consistent with results of Fig. 4.

the corresponding collapse of loop area at fixed frequency when  $H < H_c^*$  at fixed  $\Omega$ .

Our discussion focuses on a central issue: The experimental results presented in Figs. 3 and 4 and in Table I (Refs. [11] and [12]) are incompatible. The experiments on Fe/Au(100) [11] and Co/Cu(100) [12] have been interpreted as supporting dynamic scaling [Eq. (1)] with exponents  $\beta$  generally in the range covered by models referred to in Table I. Our results yield values of  $\beta$  essentially a factor of 10 smaller. Our spot-size dependent Kerr loops suggest magnetization reversal in 2–4 ML Fe on W(110) proceeds via domains on the scale of  $\sim 100 \mu\text{m}$ . Polarized electron microscopy studies [18] of 3–5 ML of Co on Cu(100) have shown that the (demagnetized film) domain structure consists of irregularly shaped domains of  $\sim 100 \mu\text{m}$ . All three systems above exhibit in-plane anisotropy. Slightly thicker Co films sandwiched between Au surfaces exhibit perpendicular anisotropy, but yield values of  $\beta$  [13,14] very similar to our results for Fe on W(110). The dynamical response of these sandwiched Co films has been analyzed using phenomenological models that assume domain nucleation and wall motion. From our discussion, it is apparent that magnetization reversal dynamics in all of the systems described here is governed by domain processes. Since the theoretical models listed in Table I do not apply to domain wall coercivity dominated magnetization reversal

processes, it is not surprising that values of  $\beta$  from our experiments do not support these models. What appears odd is the similarity of our values of  $\beta$  and those for Co/Au sandwiches [13,14] and the factor of 10 difference between our results and the experiment values in Table I.

To resolve this dilemma, we carried out experiments on the Co/Cu(100) system employing the same procedures used in our Fe/W(110) studies. We obtain temperature and frequency dependent (4 decades to 0.5 kHz) loop areas and exponents comparable to those we obtained for Fe/W(110); i.e.,  $\beta = 0.02 \pm 0.02$ . We believe that the unresolved discrepancies in dynamic exponents most likely result from subtle frequency-dependent calibrations of the magnet response. A detailed discussion of this issue will be presented in a future publication [19].

This work was supported by the NSF/DMR 9623494.

- [1] M. Rao, H.R. Krishnamurthy, and R. Pandit, Phys. Rev. B **42**, 856 (1990); M. Rao and R. Pandit, Phys. Rev. B **43**, 3373 (1991).
- [2] A. M. Somoza and R. C. Desai, Phys. Rev. Lett. **70**, 3279 (1993).
- [3] S. Sengupta, Y. Marathe, and S. Puri, Phys. Rev. B **45**, 7828 (1992).
- [4] D. Dhar and P. B. Thomas, J. Phys. A **25**, 4967 (1992); Europhys. Lett. **21**, 965 (1993).
- [5] M. Acharyya and B. K. Chakrabarti, Phys. Rev. B **52**, 6550 (1995).
- [6] W. S. Lo and R. A. Peicovits, Phys. Rev. A **42**, 7471 (1990).
- [7] F. Zhong, J. X. Zhang, and G. G. Siu, J. Phys. Condens. Matter **6**, 7785 (1994); F. Zhong and J. X. Zhang, Phys. Rev. Lett. **75**, 2027 (1995).
- [8] P. Jung, G. Gray, R. Roy, and P. Mandel, Phys. Rev. Lett. **65**, 1873 (1990).
- [9] C. N. Luse and A. Zangwill, Phys. Rev. E **50**, 224 (1994).
- [10] C. N. Luse and A. Zangwill, J. Appl. Phys. **79**, 4942 (1996).
- [11] Y.-L. He and G.-C. Wang, Phys. Rev. Lett. **70**, 2336 (1993).
- [12] Q. Jiang, H.-N. Yang, and G.-C. Wang, Phys. Rev. B **52**, 14911 (1995).
- [13] B. Raquet, R. Mamy, and J. C. Ousset, Phys. Rev. B **54**, 4128 (1996).
- [14] P. Bruno, G. Bayreuther, P. Beauvillain, C. Chappert, G. Lugert, D. Renard, J. P. Renard, and J. Seiden, J. Appl. Phys. **68**, 5759 (1990).
- [15] H. J. Elmers, Int. J. Mod. Phys. B **9**, 3115 (1995), and references therein.
- [16] J. Chen and J. L. Erskine, Phys. Rev. Lett. **68**, 1212 (1992); D.-J. Huang, J.-Y. Lee, G. A. Mulhollan, and J. L. Erskine, J. Appl. Phys. **73**, 1 (1993).
- [17] H.-P. D. Shieh and M. H. Kryder, IEEE Trans. Magn. **24**, 2464 (1988).
- [18] H. P. Oepen, J. Magn. Magn. Mater. **93**, 116 (1991).
- [19] Jih-Shin Suen, MungHee Lee, Glenn Teeter, and J. L. Erskine (to be published).